

Strongly interacting Fermi systems in $1/N$ expansion: From cold atoms to color superconductivity

Hiroaki Abuki* and Tomáš Brauner^{†‡}

*Institut für Theoretische Physik, Goethe-Universität,
Max-von-Laue-Straße 1, D-60438 Frankfurt am Main, Germany*

We investigate the $1/N$ expansion proposed recently as a strategy to include quantum fluctuation effects in the nonrelativistic, attractive Fermi gas at and near unitarity. We extend the previous results by calculating the next-to-leading order corrections to the critical temperature along the whole BCS–BEC crossover. We demonstrate explicitly that the extrapolation from the mean-field approximation, based on the $1/N$ expansion, provides a useful approximation scheme only on the BCS side of the crossover. We then apply the technique to the study of strongly interacting relativistic many-fermion systems. Having in mind the application to color superconductivity in cold dense quark matter, we develop, within a simple model, a formalism suitable to compare the effects of order parameter fluctuations in phases with different pairing patterns. Our main conclusion is that the relative correction to the critical temperature is to a good accuracy proportional to the mean-field ratio of the critical temperature and the chemical potential. As a consequence, it is significant even rather deep in the BCS regime, where phenomenologically interesting values of the quark–quark coupling are expected. Possible impact on the phase diagram of color-superconducting quark matter is discussed.

PACS numbers: 25.75.Nq, 67.85.Lm

Keywords: BCS–BEC crossover, Unitary Fermi gas, Quark matter, Color superconductivity.

I. INTRODUCTION

Strongly interacting many-fermion systems have been a theoretical challenge for decades. While the Bardeen–Cooper–Schrieffer (BCS), or mean-field (MF), theory provides an excellent description of conventional metallic superconductors, it is still inappropriate for a large range of other systems, from high-temperature superconductors to nuclear (and more recently, quark) matter.

Great theoretical interest was triggered by the conjecture that when the interaction strength is increased, BCS-type superconductivity evolves smoothly to the Bose–Einstein condensation (BEC) of tightly bound difermion molecules [1, 2, 3]. The crucial observation in this respect was that the standard BCS superconducting ground state has the same form as the ground state of a condensed Bose gas once the composite operator creating a Cooper pair is identified with that of a bosonic quasiparticle. However, in spite of the successful unified description of BCS superconductivity and BEC, a quantitative understanding of the crossover between the two regimes was missing.

Spectacular progress in this direction has been made in the past decade thanks to the experiments using ultracold atomic Fermi gases [4, 5, 6, 7]. From the theorists’ point of view, these provide an ideal tool to test the developing many-body techniques. In particular, a lot of interest has

been attracted by the transition regime between the BCS and BEC limits—the unitary Fermi gas. In this case, the two-body scattering length is much larger (ideally infinite) than any other characteristic scale of the system such as the interaction range and interparticle distance. This, on the one hand, leads to intriguing universal behavior with connections to other branches of physics such as the quark–gluon plasma or even string theory [8, 9]. On the other hand, it poses a challenging problem due to the lack of a small expansion parameter.

Several approaches have been suggested to deal with the Fermi gas at large scattering length, including various self-consistent resummation techniques for the many-body Green’s functions [10, 11] or the scattering matrix [12], expansion in the dimensionality of the space [13, 14, 15], or the $1/N$ expansion [16, 17]. An early review of the many-body approaches to the crossover problem may be found in Ref. [18]. The predictions of the analytic approximation schemes as well as the available experimental results are now being tested by increasingly precise numerical simulations [19, 20, 21, 22].

Also in high-energy physics has the mechanism of Cooper pairing proven extremely fruitful. The Nambu–Jona-Lasinio (NJL) model [23, 24], constructed in direct analogy with the BCS theory of superconductivity, was one of the first models of dynamical symmetry breaking. For its simplicity and generality, it still remains a popular low-energy effective description of strongly interacting quark and nuclear matter, this article not being an exception.

While the original NJL model dealt with dynamical breaking of chiral symmetry by particle–antiparticle correlations, the true Cooper pairing of two relativistic fermions near their Fermi surface appears in dense quark

[†]On leave from Department of Theoretical Physics, Nuclear Physics Institute ASCR, CZ-25068 Řež, Czech Republic

*Electronic address: abuki@th.physik.uni-frankfurt.de

[‡]Electronic address: brauner@ujf.cas.cz

matter, leading to the so-called color superconductivity [25, 26] (see [27] for a recent review). Due to the strong-interaction nature of quantum chromodynamics (QCD), quark matter at moderate densities is a typical example of a relativistic many-fermion system where a departure from the BCS-like behavior is to be expected. The early work in this respect focused on the structural change of Cooper pairs at strong coupling and precursor phenomena above the critical temperature for the superconducting phase transition, in particular the appearance of the pseudogap in the spectrum [28, 29, 30, 31, 32, 33].

In principle, the size of the QCD running coupling depends just on the energy/momentum scale and is thus fixed by the density of the quark matter. However, in order to better understand the strong-coupling effects in color superconductors, one often considers models with variable coupling strength where the full BCS–BEC crossover can be studied [34, 35, 36, 37, 38, 39, 40]. In the color superconductivity context, most of the calculations are still done using the MF approximation. The first attempts to include the fluctuations of the order parameter have adapted the Nozières–Schmitt-Rink (NSR) theory [3, 34, 35] and the pseudogap approximation [41], commonly used in condensed-matter physics, and the Cornwall–Jackiw–Tomboulis formalism [42, 43], well known in high-energy physics.

The goal of this paper is to investigate the applicability of the $1/N$ expansion to the study of strongly interacting Fermi gases. In Sec. II we review the $1/N$ expansion for the nonrelativistic Fermi gas developed in Refs. [16, 17]. We study the evolution of the next-to-leading-order corrections from the unitarity towards the BCS and BEC regimes and critically examine the virtues as well as shortcomings of the method. In Sec. III we then apply the technique to relativistic superconductors, using a class of NJL-type models. In particular we estimate the correction to the critical temperature in color-superconducting quark matter and show that it is significant even for realistic values of the coupling strength. On account of the fact that the fluctuation effects are different for various competing phases, we propose a modification of the QCD phase diagram. Finally, in Sec. IV we summarize and conclude.

II. NONRELATIVISTIC ATTRACTIVE FERMION GAS

We consider here the gas of two nonrelativistic fermion species (“flavors”) which will be referred to as ψ_\uparrow and ψ_\downarrow . For simplicity they will be assumed to have equal masses and chemical potentials (and thus also densities). Nevertheless, the results of the present analysis may be straightforwardly generalized to the case of a density imbalance, or, Fermi surface mismatch [17]. At low density, i.e., low characteristic momentum set by the Fermi scale, the two-body interaction is completely determined by the s -wave scattering length, a .

A. Formalism

In order to employ the $1/N$ expansion, one has to generalize the system by including N copies of the two fermion flavors. Following Refs. [16, 17], we write down the Euclidean Lagrangian in the form

$$\mathcal{L} = \sum_{i=1}^N \sum_{\sigma=\uparrow,\downarrow} \psi_{i\sigma}^\dagger \left(\partial_\tau - \frac{\nabla^2}{2m} - \mu \right) \psi_{i\sigma} - \frac{g}{N} \sum_{i,j=1}^N \psi_{i\uparrow}^\dagger \psi_{i\downarrow}^\dagger \psi_{j\downarrow} \psi_{j\uparrow}. \quad (1)$$

The sums over repeated indices will from now on be implicitly assumed. For $N = 1$ the Lagrangian reduces to one describing a two-flavor gas with local contact attractive interaction with strength g [44]. In this extended version the coupling is rescaled as $g \rightarrow g/N$ in order to ensure that the action scales naturally with N .

Note that the Lagrangian (1) possesses, apart from the phase invariance generated by the total particle number, a symplectic symmetry, $\text{Sp}(2N)$. However, as will become clear soon, this symmetry remains unbroken by the Cooper pairing so that it does not give rise to any unwanted Nambu–Goldstone (NG) bosons and hence does not affect the low-temperature thermodynamics of the system.

As a next step the theory is bosonized by introducing the auxiliary field, $\phi \sim \frac{g}{N} \psi_{i\downarrow} \psi_{i\uparrow}$, and performing the Hubbard–Stratonovich transformation. The result is the nonlocal effective action,

$$\mathcal{S} = N \int_0^\beta d\tau \int d^3\mathbf{x} \frac{|\phi(\mathbf{x}, \tau)|^2}{g} - N \text{Tr} \log \mathcal{G}^{-1}[\phi(\mathbf{x}, \tau)], \quad (2)$$

where \mathcal{G} is the Nambu-space fermion propagator in presence of the pairing field ϕ ,

$$\mathcal{G}^{-1} = \begin{pmatrix} -\partial_\tau + \frac{\nabla^2}{2m} + \mu & \phi \\ \phi^* & -\partial_\tau - \frac{\nabla^2}{2m} - \mu \end{pmatrix}.$$

Eq. (2) can be interpreted as a classical action that defines a theory of the scalar field ϕ with self-interactions determined by the expansion of the action in powers of ϕ . The crucial observation made in Refs. [16, 17] is that since the action is proportional to N , the expansion of the partition function, or the thermodynamic potential, in powers of $1/N$ is equivalent to the expansion in loops. Here and in the following, the term “loop” is used to refer to a bosonic loop, unless explicitly indicated otherwise. Note that all loops containing fermions of the original theory (1) are resummed into the action (2), i.e., are included at the tree level with respect to bosons.

Obviously, the leading order (LO) of the $1/N$ expansion is equivalent to the saddle-point approximation to the functional integral, that is, the usual MF approximation. The next-to-leading order (NLO) then incorporates one-loop corrections, or, the Gaussian fluctuations around the saddle point [45]. The $1/N$ expansion

thus provides a systematic ordering of the corrections to the MF approximation. We should nevertheless keep in mind that at the end of the calculation, we have to set $N = 1$. The way this extrapolation is performed is to be understood as a part of the definition of the method, which distinguishes it from other approaches with formally equivalent thermodynamic potential [3, 45].

In general one calculates, in a given approximation scheme, the thermodynamic potential Ω as a function of the anticipated vacuum expectation value Δ of the field ϕ , and of the chemical potential μ . Their actual values in thermodynamic equilibrium are then determined by a simultaneous solution of the gap and number equations,

$$\frac{\partial\Omega}{\partial\Delta} = 0, \quad \frac{\partial\Omega}{\partial\mu} = -n, \quad (3)$$

where n is the total particle density, related to the Fermi momentum k_F by the usual expression, $n = k_F^3/3\pi^2$. It is well known that already at one-loop level, an attempt to solve the equations self-consistently leads to unphysical results, in particular the violation of the Goldstone theorem [11]. Veillette *et al.* [17] suggested to avoid this problem by an expansion of the gap and chemical potential simultaneously with the expansion of the thermodynamic potential that follows from the action (2),

$$\begin{aligned} \Omega &= N\Omega^{(0)} + \Omega^{(1)} + \frac{1}{N}\Omega^{(2)} + \dots, \\ \Delta &= \Delta^{(0)} + \frac{1}{N}\Delta^{(1)} + \frac{1}{N^2}\Delta^{(2)} + \dots, \\ \mu &= \mu^{(0)} + \frac{1}{N}\mu^{(1)} + \frac{1}{N^2}\mu^{(2)} + \dots \end{aligned}$$

Comparing terms of the same order in the gap and number equations (3), one obtains *explicit* expressions for the higher-order corrections to the MF values $\Delta^{(0)}, \mu^{(0)}$. In particular at NLO we find

$$\begin{pmatrix} \mu^{(1)} \\ \Delta^{(1)} \end{pmatrix} = - \begin{pmatrix} \partial_{\mu\mu}\Omega^{(0)} & \partial_{\mu\Delta}\Omega^{(0)} \\ \partial_{\Delta\mu}\Omega^{(0)} & \partial_{\Delta\Delta}\Omega^{(0)} \end{pmatrix}^{-1} \begin{pmatrix} \partial_{\mu}\Omega^{(1)} \\ \partial_{\Delta}\Omega^{(1)} \end{pmatrix}. \quad (4)$$

It is essential that all derivatives of the thermodynamic potential here are evaluated using the MF values $\Delta^{(0)}, \mu^{(0)}$. One thus avoids the problems with self-consistency; in particular the NG boson of the spontaneously broken symmetry is exactly massless [16].

When we merely wish to determine the critical temperature, the gap in Eq. (3) is fixed to zero and we solve for the temperature and chemical potential instead. The identity (4) then naturally modifies to one for the corrections of the variables of interest,

$$\begin{pmatrix} \mu_c^{(1)} \\ T_c^{(1)} \end{pmatrix} = - \begin{pmatrix} \partial_{\mu\mu}\Omega^{(0)} & \partial_{\mu T}\Omega^{(0)} \\ \partial_{\Delta\mu}\Omega^{(0)} & \partial_{\Delta T}\Omega^{(0)} \end{pmatrix}^{-1} \begin{pmatrix} \partial_{\mu}\Omega^{(1)} \\ \partial_{\Delta}\Omega^{(1)} \end{pmatrix}. \quad (5)$$

We will comment later on the ambiguity that arises at this point, stemming from the fact that we can choose to solve Eq. (3) for $1/T_c$ (or any other function of T_c)

and accordingly get a different type of $1/N$ expansion— all derivatives with respect to T in Eq. (5) would simply turn into ones with respect to $1/T$.

Eqs. (4) and (5) of course have to be supplemented with an expression for the thermodynamic potential. For the sake of this section, we will need just the explicit form of the standard MF part,

$$\begin{aligned} \Omega^{(0)} &= \frac{|\Delta|^2}{g} - \int \frac{d^3\mathbf{k}}{(2\pi)^3} (E_{\mathbf{k}} - \xi_{\mathbf{k}}) \\ &\quad - 2T \int \frac{d^3\mathbf{k}}{(2\pi)^3} \log(1 + e^{-\beta E_{\mathbf{k}}}), \end{aligned} \quad (6)$$

using the usual notation $\epsilon_{\mathbf{k}} = \frac{\mathbf{k}^2}{2m}$, $\xi_{\mathbf{k}} = \epsilon_{\mathbf{k}} - \mu$, and $E_{\mathbf{k}} = \sqrt{\xi_{\mathbf{k}}^2 + |\Delta|^2}$. The bare coupling g is related to the physical scattering length by

$$\frac{1}{g} = -\frac{m}{4\pi a} + \int \frac{d^3\mathbf{k}}{(2\pi)^3} \frac{1}{2\epsilon_{\mathbf{k}}}. \quad (7)$$

For further details, we refer the reader to the original literature [16, 17] where all necessary formulas are derived in detail. In Sec. III we will develop a relativistic formalism from which the present case will follow as a particular nonrelativistic limit.

B. Numerical results

1. Critical temperature

While differing in other specific directions of investigation, both Refs. [16, 17] addressed the question of special interest, the calculation of the critical temperature at unitarity. Veillette *et al.* obtained the result

$$\frac{T_c}{\epsilon_F} = 0.4964 - \frac{1.31}{N} \quad (8)$$

in units of the Fermi energy, $\epsilon_F = k_F^2/2m$, whereas Nikolić and Sachdev calculated the correction to the inverse temperature and got

$$\frac{\epsilon_F}{T_c} = 2.014 + \frac{5.317}{N}. \quad (9)$$

Both results are formally equivalent to order $1/N$ in the expansion, yet they yield dramatically different numbers when evaluated at $N = 1$. Indeed, Eq. (8) becomes even meaninglessly negative and can be merely used to make the qualitative conclusion that the fluctuations decrease the critical temperature significantly.

On the other hand, Eq. (9) leads to the critical temperature $T_c = 0.14\epsilon_F$ in remarkable agreement with the result $T_c = 0.152(7)\epsilon_F$, obtained by numerical Monte Carlo simulations [21, 22]. However, it should be stressed that there is no *a priori* criterion that would tell us which observable to choose for the evaluation of the NLO correction. One may think that it is the Lagrange multiplier

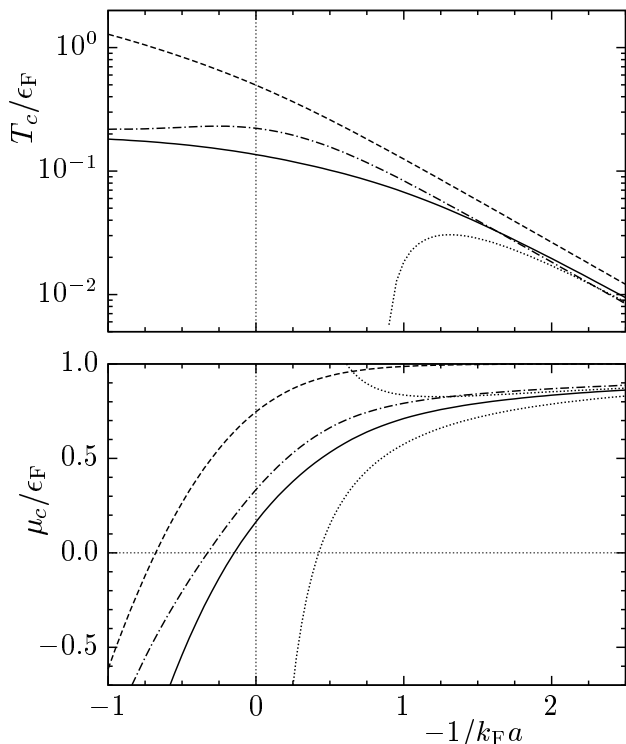


FIG. 1: Critical temperature and chemical potential as a function of the inverse scattering length. Dashed lines: MF approximation (LO in $1/N$). Solid lines: NLO calculation based on expansion of $1/T$. Dotted line in the upper panel: NLO value based on expansion of T as in Eq. (5). Dash-dotted lines: Self-consistent calculation using NSR theory. Dotted lines in the lower panel: First- and second-order perturbative approximations to the chemical potential, see Eq. (10).

$\beta = 1/T$ rather than the temperature itself that is the natural variable of the thermodynamic potential. Still a deeper physical argument is obviously needed to resolve this ambiguity. Here we just remark that on the technical level, it clearly arises from the truncation of the $1/N$ series for different observables; one cannot expect the $1/N$ expansion to be reliable when the NLO term is larger than the LO one [59].

In order to further study the size of the $1/N$ corrections and the sensitivity to the choice of observable to evaluate them, we calculated the critical temperature at NLO as a function of the inverse scattering length, see Fig. 1.

Obviously, the evaluation of the critical temperature based on Eq. (5) (dotted line in the upper panel) is only reasonable in the far BCS regime (right end of the plot) where it roughly coincides with the $1/T$ -based approximation (solid line). The $1/T$ -based value will therefore be used exclusively in the following and will be referred to simply as the NLO critical temperature. For comparison we also show the critical temperature and chemical potential calculated using the NSR theory (dash-dotted line). NSR theory takes the fluctuation effects into account only in the total particle number, but not in the

gap equation. On the other hand, it then solves Eq. (3) self-consistently [60].

In the BCS regime the critical temperatures calculated within the two approaches are consistent with each other, at least qualitatively. Around unitarity, NSR theory predicts a well-known tiny maximum. On the contrary, the $1/N$ expansion gives a monotonic dependence on the inverse scattering length, with the value at unitarity agreeing very well with Monte Carlo calculations [21, 22], as noted above. However, as also emphasized there, the $1/N$ expansion should not be really trusted in this region without an additional physical insight. Finally, in the BEC limit NSR theory converges to the expected critical temperature of the free Bose gas, $T_c = 0.218\epsilon_F$. $1/N$ expansion fails to reproduce this asymptotic behavior. Although it cannot be seen in Fig. 1, its critical temperature keeps growing towards the BEC limit, albeit with a decreasing slope. Indeed, one cannot really expect to get a constant asymptotics from a perturbative expansion around the rapidly increasing MF value.

In the lower panel of Fig. 1 we also display the results for the chemical potential at the critical temperature. Here the most interesting is the evolution in the far BCS region. While in the MF approximation the chemical potential approaches its asymptotic value equal to the Fermi energy with an exponentially decreasing tail, upon including fluctuations the convergence turns into a much slower, power-law one. This is a purely perturbative effect, as clearly demonstrated by a comparison with the standard perturbative expansion for the chemical potential in the dilute Fermi gas [46] (the first- and second-order values are plotted using dotted lines)

$$\frac{\mu}{\epsilon_F} = 1 + \frac{4}{3\pi}k_F a + \frac{4(11 - 2 \log 2)}{15\pi^2}(k_F a)^2 + \dots \quad (10)$$

Even though this formula holds only in the normal phase and at zero temperature, the agreement is excellent. The reason, of course, is that the pairing effects are suppressed exponentially and finite-temperature effects are also suppressed by the exponentially small value of the critical temperature in the BCS limit, so that they are both completely negligible with respect to the perturbative corrections in Eq. (10) [45].

The fact that the NLO in $1/N$ reproduces the perturbative expansion of the chemical potential up to second order can also be verified directly on the Feynman graph level. In Fig. 2 we show the perturbative contributions to the thermodynamic potential. In general the $1/N$ expansion does not coincide with perturbation series—the diagram (d) is of second order in the interaction, yet only appears at the next-to-next-to-leading order in $1/N$. Fortunately, it turns out to vanish at zero temperature so that the $1/N$ expansion to NLO indeed contains the full second-order perturbative correction [47].

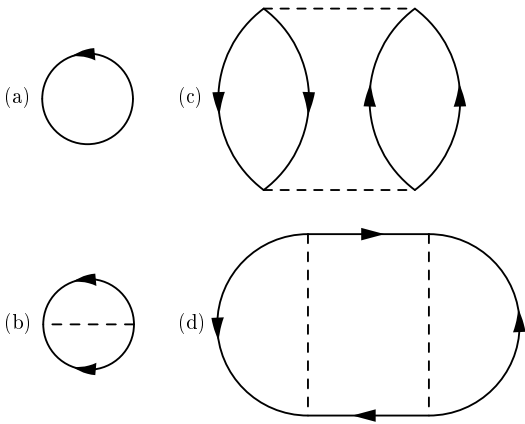


FIG. 2: Lowest-order perturbative contributions to the thermodynamic potential of the Fermi gas. The free-gas graph (a) coincides with LO in $1/N$. The first-order graph (b) and the second-order graph (c) appear at NLO in $1/N$. The second-order graph (d) contributes only at NNLO. The dashed line denotes the bare propagator of the pairing field ϕ , g/N .

2. BCS limit

Since we have concluded that the $1/N$ expansion is most reliable on the BCS side of the crossover, let us now investigate this regime in more detail. The matrix of second derivatives of $\Omega^{(0)}$ at the critical temperature needed to evaluate the NLO corrections $\beta^{(1)}$ and $\mu^{(1)}$ can be easily calculated from Eq. (6). One finds

$$\begin{aligned} \partial_{\mu\mu}\Omega^{(0)} &= -\frac{3n}{2\epsilon_F}, & \partial_{\mu\beta}\Omega^{(0)} &= \frac{\pi^2 n T^3}{4\epsilon_F^2}, \\ \partial_{\Delta^2\beta}\Omega^{(0)} &= -\frac{3nT}{4\epsilon_F}, \end{aligned}$$

up to corrections which are exponentially small as $k_F a \rightarrow 0^-$. (Note that we prefer to take the derivative with respect to Δ^2 instead of Δ since at the critical temperature we have to set $\Delta = 0$ afterwards.) The last needed coefficient,

$$\partial_{\Delta^2\mu}\Omega^{(0)} = \frac{3n}{4\epsilon_F^2} \left(\frac{\pi}{4k_F a} - 1 \right),$$

is most easily obtained using the exact relation

$$\partial_{\Delta^2\beta}\Omega^{(0)} = -\frac{3\pi n T}{16\epsilon_F k_F a} + \mu T \partial_{\Delta^2\mu}\Omega^{(0)},$$

which follows from the observation that $\Omega^{(0)}$ can be expressed in terms of a dimensionless function of the combination $\beta\mu$.

The coefficient $\partial_{\mu\beta}\Omega^{(0)}$ is strongly suppressed by the third power of the critical temperature so that it may be neglected and the required matrix of second derivatives

[as in Eq. (5), just with modified variables] becomes

$$\begin{aligned} & \begin{pmatrix} \partial_{\mu\mu}\Omega^{(0)} & \partial_{\mu\beta}\Omega^{(0)} \\ \partial_{\Delta^2\mu}\Omega^{(0)} & \partial_{\Delta^2\beta}\Omega^{(0)} \end{pmatrix}^{-1} \\ & \approx \frac{1}{\partial_{\mu\mu}\Omega^{(0)}\partial_{\Delta^2\beta}\Omega^{(0)}} \begin{pmatrix} \partial_{\Delta^2\beta}\Omega^{(0)} & 0 \\ -\partial_{\Delta^2\mu}\Omega^{(0)} & \partial_{\mu\mu}\Omega^{(0)} \end{pmatrix}. \end{aligned}$$

As a result, the leading NLO contribution to the chemical potential decouples and is solely determined by $\partial_{\mu}\Omega^{(1)}$ and $\partial_{\mu\mu}\Omega^{(0)}$,

$$\mu_c^{(1)} = -\frac{\partial_{\mu}\Omega^{(1)}}{\partial_{\mu\mu}\Omega^{(0)}}.$$

This is not surprising since we know from Eq. (10) that in the BCS limit the chemical potential is governed by perturbative effects. The expression for the shift of the inverse critical temperature also simplifies to

$$\beta_c^{(1)} = -\frac{\partial_{\Delta^2}\Omega^{(1)} + \mu_c^{(1)}\partial_{\Delta^2\mu}\Omega^{(0)}}{\partial_{\Delta^2\beta}\Omega^{(0)}}.$$

Substituting all the analytic expressions listed above as well as the chemical potential correction from Eq. (10) we get the final prediction of the $1/N$ expansion for the NLO relative shift of the inverse temperature in the BCS limit,

$$\frac{\beta_c^{(1)}}{\beta_c^{(0)}} = \frac{4\epsilon_F}{3n}\partial_{\Delta^2}\Omega^{(1)} + \frac{1}{3} \left(1 - \frac{9 + 2 \log 2}{5\pi} k_F a \right),$$

where the only missing ingredient, that has to be evaluated numerically, is $\partial_{\Delta^2}\Omega^{(1)}$.

The point of these considerations is that the slow, perturbative convergence of the chemical potential results in a rather large offset in the critical temperature, which *survives* even in the limit $k_F a \rightarrow 0^-$. This is a consequence of the fact that $\partial_{\Delta^2\mu}\Omega^{(0)}$ diverges in the BCS limit; we regard it an artifact of the expansion of the gap and number equations, leading to the expression (4).

In addition to the critical temperature, we have also computed the gap and chemical potential at zero temperature, see Fig. 3. This has already been done by Veillette *et al.* [17], although they did not investigate the asymptotic behavior in the BCS limit. Our calculation differs from theirs only in that we have for technical reasons taken Δ^2 instead of Δ as the variable to make the $1/N$ expansion. Since the relative NLO correction to the gap at zero temperature is small, the effect of this change is nearly negligible.

Fig. 3 suggests that the gap also acquires a constant offset that survives the BCS limit (even though we were not able to check this conclusion analytically). However, the offset is not the same as in the case of the critical temperature, as is clearly seen from Fig. 4 where we plot the ratio T_c/Δ_0 . Thus, $1/N$ expansion predicts a departure of this ratio from the BCS value e^γ/π . In Sec. III we will present a calculation of the critical temperature within a $1/N$ -inspired high-density approximation, where such artifacts will be absent.

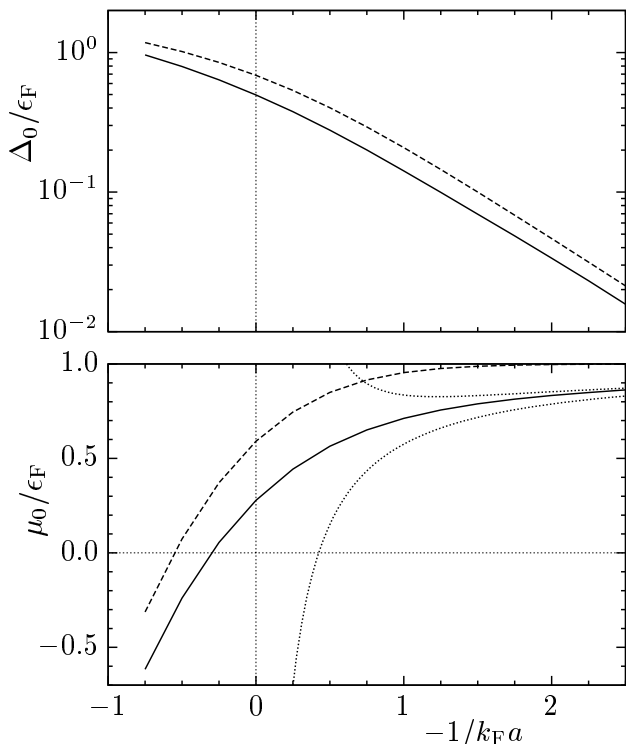


FIG. 3: Gap and chemical potential at zero temperature as a function of the inverse scattering length. Dashed lines: MF approximation (LO in $1/N$). Solid lines: NLO calculation based on expansion of Δ^2 . Dotted lines in lower panel: First- and second-order perturbative approximations to the chemical potential, see Eq. (10).

III. DENSE RELATIVISTIC MATTER

We are now going to apply the $1/N$ expansion to pairing in relativistic systems. Physically, this amounts to including the antiparticles among the degrees of freedom, and to modifying the fermion dispersion relation. In particular the change of dispersion relation affects the ultraviolet structure of the theory, leading to new divergences that are not present in the nonrelativistic case [35]. In Sec. III B we evade this difficulty by making a suitable approximation, appropriate in the far BCS regime.

A. NJL-type model

Following closely the notation of Ref. [39], we consider a class of NJL-type models defined by the Lagrangian

$$\mathcal{L} = \bar{\psi}(i\not{\partial} + \mu\gamma_0 - m)\psi + \frac{g}{4} \sum_a |\bar{\psi}^c \gamma_5 Q_a \psi|^2, \quad (11)$$

where $\psi^c = C\bar{\psi}^T$ is the standard charge-conjugated Dirac spinor and the set of matrices Q_a , acting on the internal degrees of freedom, are normalized by $\text{Tr}(Q_a Q_b^\dagger) = \delta_{ab}$. Simplified as much as possible, this Lagrangian

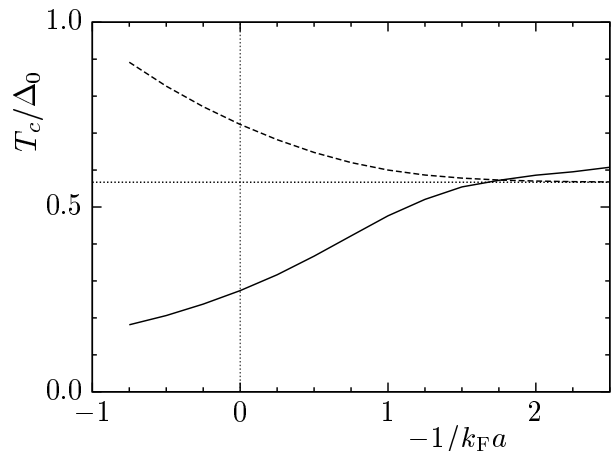


FIG. 4: Ratio of the critical temperature to the gap at zero temperature as a function of the inverse scattering length. Dashed line: MF approximation. Solid line: NLO calculation with data taken from Figs. 1 and 3. Horizontal dotted line: Prediction of the BCS theory.

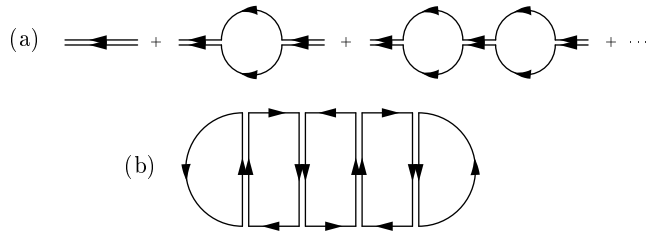


FIG. 5: (a) RPA propagator of the collective mode in the case it transforms as an antisymmetric tensor of $SU(N)$, using the double-line notation. (b) One of the planar diagrams which dominate the thermodynamic potential in the large- N limit.

describes a system of interacting fermions with equal masses and chemical potentials. The pairing is assumed to occur in a spin-zero, positive-parity channel, but its flavor structure, determined by the matrices Q_a , can be arbitrary. Once we understand in detail the fluctuation effects in this simple setting, we will move on to more realistic systems in our future work.

The first task to solve is the generalization of the model to arbitrary N so that we can subsequently make the appropriate expansion. With the application to quark matter in mind, one may think it would be most convenient to use the color $SU(3)$ symmetry already present in the system and extend it to $SU(N)$. We would like to explain here in detail why this would not work.

As a consequence of the QCD interactions, quarks are assumed to pair in a color-antisymmetric configuration. (Symmetry would not make a difference. Important is that the Cooper pair cannot be a singlet of the symmetry due to the complex nature of the group $SU(3)$.) Upon the generalization of the theory the pairs would transform in the antisymmetric-tensor representation of $SU(N)$. Disregarding the fact that this would lead to a

very large number, of order $\mathcal{O}(N^2)$, of collective modes, there is another, more serious problem.

In Sec. II we saw using the scaling of the thermodynamic potential that the $1/N$ expansion reproduces the MF approximation at the leading order. This may be also understood in terms of the collective mode propagator. In the MF approximation, this consists of a geometric series of graphs in the random-phase approximation (RPA). Now since the boson is a singlet of the $\text{Sp}(2N)$ symmetry, each fermion bubble contributes a factor N from the trace over the flavor space, thus compensating for factors $1/N$ coming from the coupling g . The point is that when the boson becomes a tensor of $\text{SU}(N)$ rather than a singlet, the trace factors are lost, as is most easily visualized with the help of the double-line notation, see Fig. 5 (a). As a consequence, addition of each new fermion bubble in the RPA series suppresses the graph by another factor $1/N$ from the coupling so that the full series will not be resummed at any finite order in $1/N$.

Is it then possible to make the coupling scale just as $\mathcal{O}(1)$? No, because the thermodynamic potential is dominated by the planar diagrams with a single fermion loop (rather than the RPA ones), which contain the same number of flavor traces as the coupling factors, see Fig. 5 (b). So, in order that the power of N in Feynman graphs is bounded from above and the $1/N$ expansion makes sense at all, the coupling has to decrease at least as $1/N$.

We thus conclude that when the difermion field is defined to be a tensor of the $\text{SU}(N)$ color group, we will not get the RPA propagator and hence the pairing instability at any finite order in $1/N$. The $1/N$ expansion in this case efficiently resums a different class of diagrams than necessary. To remedy this problem, we introduce a new quantum number to label the fermion fields, i.e., generalize Eq. (11) to

$$\mathcal{L} = \bar{\psi}_i (i\cancel{\partial} + \mu\gamma_0 - m)\psi_i + \frac{g}{4N} \sum_a |\bar{\psi}_i^c \gamma_5 Q_a \psi_i|^2. \quad (12)$$

This has two advantages. First, one does not need to rely on the presence of the color $\text{SU}(3)$. The construction is absolutely general, regardless of the actual physical internal degrees of freedom. Second, the Cooper pair is a singlet with respect to the symmetry transformations acting on the new quantum number so that there are no additional bosonic degrees of freedom introduced by the extension of the symmetry and no unwanted NG bosons from its spontaneous breaking. On the other hand one has to set, just like in the nonrelativistic case, $N = 1$ at the end of the calculation.

With the above argument in mind, we proceed as in Sec. II. Upon bosonization of the theory (12) by introducing a set of auxiliary fields, $\phi_a \sim \frac{g}{2N} \bar{\psi}_i^c \gamma_5 Q_a \psi_i$, we arrive at the effective action

$$\mathcal{S} = N \int_0^\beta d\tau \int d^3\mathbf{x} \frac{|\phi_a(\mathbf{x}, \tau)|^2}{g} - N \text{Tr} \log \mathcal{G}^{-1}[\phi_a(\mathbf{x}, \tau)], \quad (13)$$

with the inverse fermion propagator in the Nambu space given by

$$\mathcal{G}^{-1} = \begin{pmatrix} i\cancel{\partial} + \gamma_0\mu - m & -\phi_a \gamma_5 Q_a^\dagger \\ \phi_a^* \gamma_5 Q_a & i\cancel{\partial} - \gamma_0\mu - m \end{pmatrix}.$$

From the classical action (13) we can generate the LO (RPA) propagator of the collective bosonic modes by a second functional derivative. Within this paper, we will for simplicity restrict our attention to the normal phase; the extension of the formalism below the critical temperature will be considered elsewhere. In the normal phase, the LO boson propagator becomes $\mathcal{D}_{0ab} = \mathcal{D}_0 \delta_{ab}$,

$$\frac{1}{N} \mathcal{D}_0^{-1}(i\omega_n, \mathbf{p}) = \frac{1}{g} + \frac{1}{2} \int \frac{d^3\mathbf{k}}{(2\pi)^3} \left\{ \left[1 + \frac{m^2 + \mathbf{k}_+ \cdot \mathbf{k}_-}{\epsilon_{\mathbf{k}_+} \epsilon_{\mathbf{k}_-}} \right] \left[\frac{f(\epsilon_{\mathbf{k}_+} + \mu) + f(\epsilon_{\mathbf{k}_-} + \mu) - 1}{i\omega_n + 2\mu + \epsilon_{\mathbf{k}_+} + \epsilon_{\mathbf{k}_-}} + \frac{1 - f(\epsilon_{\mathbf{k}_+} - \mu) - f(\epsilon_{\mathbf{k}_-} - \mu)}{i\omega_n + 2\mu - \epsilon_{\mathbf{k}_+} - \epsilon_{\mathbf{k}_-}} \right] \right. \\ \left. + \left[1 - \frac{m^2 + \mathbf{k}_+ \cdot \mathbf{k}_-}{\epsilon_{\mathbf{k}_+} \epsilon_{\mathbf{k}_-}} \right] \left[\frac{f(\epsilon_{\mathbf{k}_+} + \mu) - f(\epsilon_{\mathbf{k}_-} - \mu)}{i\omega_n + 2\mu + \epsilon_{\mathbf{k}_+} - \epsilon_{\mathbf{k}_-}} + \frac{f(\epsilon_{\mathbf{k}_-} + \mu) - f(\epsilon_{\mathbf{k}_+} - \mu)}{i\omega_n + 2\mu + \epsilon_{\mathbf{k}_-} - \epsilon_{\mathbf{k}_+}} \right] \right\}, \quad (14)$$

where $\mathbf{k}_\pm = \mathbf{k} \pm \frac{\mathbf{p}}{2}$ and $f(x) = 1/(e^{\beta x} + 1)$ is the Fermi-Dirac distribution function.

Assuming that the order parameter fluctuations do not change the second order of the phase transition, we can find the critical temperature using the Thouless criterion [48], i.e., by requiring that the normal-phase boson propagator has a pole (pairing singularity) at zero (four-)momentum. This is equivalent to the gap equation $\partial\Omega/\partial\Delta^2 = 0$ at $\Delta = 0$. The expression $\partial\Omega^{(1)}/\partial\Delta^2$ that

appears in the NLO formula for the critical point (5), is thus seen to represent the one-loop boson self-energy at zero momentum.

In a general scalar self-interacting theory the one-loop self-energy is given by the tadpole diagram with one quartic interaction vertex. In case of the theory defined by the action (13), the effective four-boson vertex is generated by a fermion loop, see Fig. 6. Let us concentrate on the flavor structure of the diagram. Assuming that

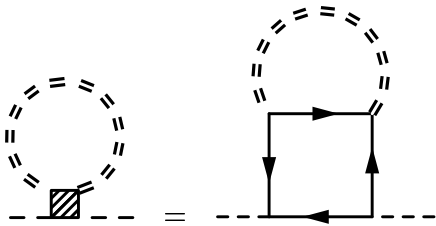


FIG. 6: One-boson-loop contribution to the collective mode self-energy. The double-dashed line denotes the resummed LO boson propagator.

the external scalar legs carry the flavor indices a, b , the complete information about the pairing pattern will be encoded in the flavor trace $\delta_{cd} \text{Tr}_F(Q_a Q_b^\dagger Q_c Q_d^\dagger)$, the Kronecker delta coming from the internal boson propagator. The combination $\delta_{cd} Q_c Q_d^\dagger$ is the quadratic Casimir operator of the symmetry group in the representation of the Cooper pairs, and therefore must be proportional to the unit matrix as long as this representation is irreducible, i.e., we consider a single pairing channel [61]. Writing $\delta_{cd} Q_c Q_d^\dagger = C_2 \mathbb{1}$ and taking the trace, we immediately find that $C_2 = \delta_{cd} \delta_{cd} / \text{dim}(Q)$, where $\text{dim}(Q)$ denotes the size of the matrices Q_a . To conclude the argument we just note that this is equal to the number of internal

fermionic degrees of freedom, N_F , while $\delta_{cd} \delta_{cd}$ counts the number of bosonic degrees of freedom, N_B . The whole effect of the structure of the symmetry group will thus be the simple algebraic prefactor,

$$\delta_{cd} \text{Tr}_F(Q_a Q_b^\dagger Q_c Q_d^\dagger) = \frac{N_B}{N_F} \delta_{ab}.$$

The full expression for the inverse boson propagator with one-loop correction then reads

$$\mathcal{D}^{-1}(P) = \mathcal{D}_0^{-1}(P) + N \frac{N_B}{N_F} \oint dK dQ \mathcal{D}_0(Q) \times \text{Tr}[\gamma_5 \mathcal{G}_{11}(K+P) \gamma_5 \mathcal{G}_{22}(K) \gamma_5 \mathcal{G}_{11}(K+Q) \gamma_5 \mathcal{G}_{22}(K)],$$

where the subscripts 11 and 22 refer to the matrix structure of the fermion propagator in the Nambu space. For the sake of brevity we used the notation for the four-momentum, $P = (i\omega_n, \mathbf{p})$, and the sum-integral,

$$\oint dK = T \sum_n \int \frac{d^3 \mathbf{k}}{(2\pi)^3}.$$

For zero external momentum the Matsubara sum in the fermion loop may easily be done and we arrive at the final analytic result,

$$\mathcal{D}^{-1}(0) = \mathcal{D}_0^{-1}(0) + N \frac{N_B}{N_F} \oint dQ \mathcal{D}_0(Q) \sum_{e,f=\pm} \int \frac{d^3 \mathbf{k}}{(2\pi)^3} \left[1 + ef \frac{m^2 + \mathbf{k} \cdot (\mathbf{k} + \mathbf{q})}{\epsilon_{\mathbf{k}} \epsilon_{\mathbf{k}+\mathbf{q}}} \right] I(e\xi_{\mathbf{k}}^e, f\xi_{\mathbf{k}+\mathbf{q}}^f; i\Omega_n), \quad (15)$$

$$I(a, b; i\Omega_n) = \frac{1}{8a^2} \frac{\tanh \frac{\beta a}{2} + \tanh \frac{\beta b}{2} - \beta a \cosh^{-2} \frac{\beta a}{2}}{i\Omega_n + b + a} + \frac{1}{8a^2} \frac{\tanh \frac{\beta a}{2} - \tanh \frac{\beta b}{2}}{i\Omega_n + b - a} + \frac{1}{4a} \frac{\tanh \frac{\beta a}{2} + \tanh \frac{\beta b}{2}}{(i\Omega_n + b + a)^2},$$

with the usual relativistic notation, $\epsilon_{\mathbf{k}} = \sqrt{\mathbf{k}^2 + m^2}$, $\xi_{\mathbf{k}}^e = \epsilon_{\mathbf{k}} + e\mu$. Note that upon taking the nonrelativistic limit, that is, including only particle degrees of freedom (with $e = f = -$), shifting the chemical potential to $\mu_{\text{NR}} = \mu - m$, and approximating the dispersion relation with $\epsilon_{\mathbf{k}} = m + \frac{\mathbf{k}^2}{2m}$, we reproduce the expression for the one-loop propagator correction given by Nikolić and Sachdev [16].

B. High-density approximation

The nonrelativistic limit of Eq. (15) may be used directly to calculate the NLO corrections to the critical temperature and chemical potential via Eq. (5). To that end, we need to supplement Eq. (15) with an analogous one-loop correction to particle density, which in turn yields the term $\partial_\mu \Omega^{(1)}$ in Eq. (5). This is how the results presented in Fig. 1 were obtained.

On the contrary, in the full relativistic description the

one-loop term in Eq. (15) is badly divergent. This is, of course, no surprise since in a relativistic scalar self-interacting field theory the one-loop tadpole graph has a quadratic divergence. Nevertheless, this divergence has nothing in common with the many-body physics, and can be removed by renormalizing the parameters of the theory in the vacuum. In order to avoid this complication and also the interference of all energy scales from the high-energy vacuum physics down to the scale of Cooper pairing, we resort to a high-density approximation [49], which is appropriate in the far BCS region where the pairing energy scale is well separated from the Fermi scale. This approximation is at the MF level known to soften the ultraviolet divergences and give some cutoff-independent predictions such as the universal BCS ratio of the gap at zero temperature and the critical temperature [50].

In our one-loop calculation we have to be more careful. We therefore spell explicitly all simplifying assumptions that we make. First, we neglect antiparticle contribu-

tions. This can be appropriate even in the ultrarelativistic limit as long as the pairing gap/critical temperature is much smaller than the Fermi energy so that the relevant excitations are the quasiparticles and quasiholes near the Fermi surface. In a strongly coupled relativistic superconductor, the antiparticle effects may be non-negligible [40] but will not change our conclusions qualitatively.

Second, we approximate, as usual, the volume measure for the integral over fermionic momentum by

$$\int \frac{d^3\mathbf{k}}{(2\pi)^3} \rightarrow \mathcal{N} \int d\xi \int \frac{d\Omega_{\mathbf{k}}}{4\pi},$$

where $\xi \equiv \xi_{\mathbf{k}}^-$ is the energy with respect to the Fermi level and $\mathcal{N} = \mu k_F / 2\pi^2$ is the density of states on the Fermi surface. This brings in one subtlety. In a nonrenormalizable theory such as the NJL model, there is an inherent ambiguity in the way we label internal propagators of the Feynman graphs with momenta which satisfy momentum conservation in the interaction vertices. For instance, in the one-loop pairing susceptibility (14) one often labels the propagators with $\mathbf{k}, \mathbf{k} \pm \mathbf{p}$ instead of $\mathbf{k} + \frac{\mathbf{p}}{2}, \mathbf{k} - \frac{\mathbf{p}}{2}$ used here, and imposes a cutoff on the loop momentum \mathbf{k} . This ambiguity can be removed by a proper renormalization which makes the graph finite. However, once we make the above introduced replacement of the integration measure in the high-density approximation, the new measure is no longer translationally invariant. That is, *the result depends on the momentum assignment to the propagators* even in an otherwise finite loop integral. In Eq. (14) we chose the symmetric momentum assignment because it reduces cutoff dependence of the result and also leads to a physically intuitive suppression of the high-momentum pair modes by Pauli blocking.

Third and most importantly, in order to retain in the calculation only the physically relevant degrees of freedom, we cut off the ξ integration at the pairing scale, $|\xi| \leq \Lambda$. In quark matter, such a cutoff is effectively introduced in terms of the momentum-dependent gap function by solving the QCD Schwinger–Dyson equations [51]. In addition, a cutoff much smaller than the Fermi energy is necessary in order to make the high-density approximation consistent [49]. In practice, we verify that the results are not sensitive to a precise value of the cutoff by doing all calculations for two different values, $\Lambda = 2T_c^{(0)}$ and $\Lambda = 4T_c^{(0)}$.

Fourth, once we restrict ourselves to the low-energy excitations about the Fermi surface, we expand the dispersion relations in terms of the Fermi velocity and an “effective mass”. This allows us to introduce efficiently dimensionless variables and treat on the same footing the non-relativistic (NR) limit of Sec. II as well as the opposite-extreme, ultrarelativistic (UR) limit of zero fermion mass (which is a reasonable approximation for quark matter composed solely of the u and d flavors). Concretely, taking the LO critical temperature $T_c^{(0)}$ as a unit for the energy variables and $T_c^{(0)}/v_F$, where v_F is the Fermi velocity, as a unit for external momentum, the dispersions

in the two opposite limits acquire very similar forms,

$$\begin{aligned} \bar{\xi}_{\mathbf{k}+\mathbf{p}} &= \bar{\xi}_{\mathbf{k}} + |\bar{\mathbf{p}}| \cos \theta + \frac{\bar{\mathbf{p}}^2}{4} \frac{T_c^{(0)}}{\mu}, & \text{NR limit,} \\ \bar{\xi}_{\mathbf{k}+\mathbf{p}} &= \bar{\xi}_{\mathbf{k}} + |\bar{\mathbf{p}}| \cos \theta + \frac{\bar{\mathbf{p}}^2}{2} \frac{T_c^{(0)}}{\mu} \sin^2 \theta, & \text{UR limit,} \end{aligned}$$

where $\bar{\xi} = \xi/T_c^{(0)}$ and $\bar{\mathbf{p}} = \mathbf{p}v_F/T_c^{(0)}$, θ is the angle between the vectors \mathbf{k} and \mathbf{p} , and the nonrelativistic chemical potential is understood in the first line, without specifying the subscript _{NR} in the following. Using this procedure, all integrals would factorize into a product of powers of the temperature and Fermi velocity and a universal dimensionless function of the ratio $T_c^{(0)}/\mu$, were it not for the coupling g .

The last step in the construction therefore has to be the renormalization of the bare coupling. In the context of atomic gases near unitarity it is customary to do this by fixing the s -wave scattering length at zero momentum in the vacuum as in Eq. (7). However, in an effective description near the Fermi surface, this is no longer convenient. We therefore renormalize the bare coupling with the help of the gap equation at zero temperature, which has the same divergence structure as the inverse propagator (14). This is effectively done by the replacement

$$\begin{aligned} \frac{1 - f(\xi_{\mathbf{k}_+}) - f(\xi_{\mathbf{k}_-})}{i\omega_n - \xi_{\mathbf{k}_+} - \xi_{\mathbf{k}_-}} \\ \rightarrow \frac{1 - f(\xi_{\mathbf{k}_+}) - f(\xi_{\mathbf{k}_-})}{i\omega_n - \xi_{\mathbf{k}_+} - \xi_{\mathbf{k}_-}} + \frac{1}{2\sqrt{\xi_{\mathbf{k}}^2 + \Delta_0^2}} \end{aligned}$$

in the inverse propagator (14) in the high-density approximation. Now everything is expressed in terms of the dimensionless ratios $T_c^{(0)}/\mu$ and $T_c^{(0)}/\Delta_0$. The ratio $T_c^{(0)}/\mu$ is used as the input parameter which measures the strength of the interaction. The ratio $T_c^{(0)}/\Delta_0$ is equal to the BCS value $\frac{e\gamma}{\pi} \approx 0.567$ in the infinite-cutoff limit. With the explicit cutoff on the ξ -integration, we adjust the value of Δ_0 appropriately in order to ensure that the Goldstone theorem is satisfied and the propagator (14) has an exactly massless pole.

Due to the explicit cutoff, the loop part of the inverse propagator (14) drops rapidly for external momenta larger than the cutoff as a result of Pauli blocking. The boson propagator approaches a constant value, equal to g/N . This is natural: At large momentum, pairing fluctuations are suppressed and the auxiliary field propagator recovers the original contact four-fermion interaction. In order that we really include just the effect of the fluctuations of the order parameter, we make in the second term of Eq. (15) the replacement

$$\mathcal{D}_0(Q) \rightarrow \mathcal{D}_0(Q) - \frac{g}{N}.$$

In terms of Feynman graphs, this means removing from the RPA series of diagrams the first, constant term, keeping all other terms that involve multiple rescattering of

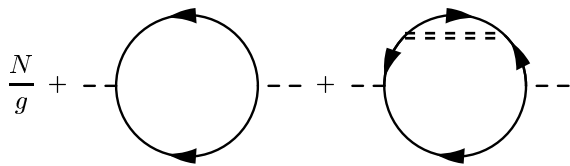


FIG. 7: Sum of the LO and NLO contributions to the inverse boson propagator. The asymptotically constant part of the fermion self-energy in the second diagram may be absorbed in a perturbative renormalization of the Fermi energy.

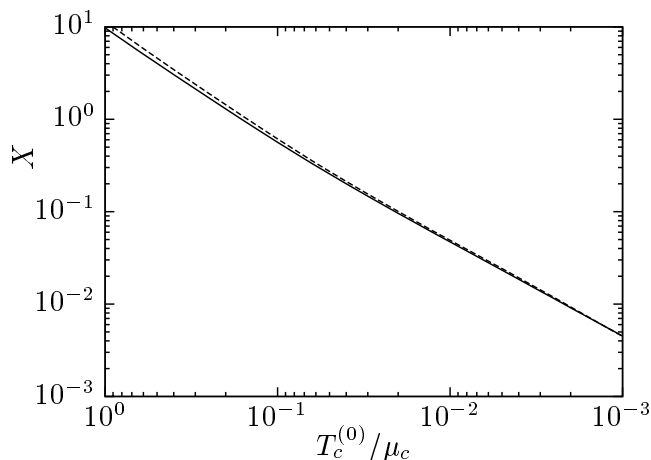


FIG. 8: Correction to the critical temperature calculated using the high-density approximation in the *nonrelativistic limit*. The calculation was done with the cutoff on fermion energy variable set to $2T_c^{(0)}$ (solid line) and $4T_c^{(0)}$ (dashed line).

the two fermions in the pair. Formally, this subtraction can be justified by observing that the diagram in Fig. 6 may also be viewed as a fermion loop with the insertion of a one-loop fermion self-energy, see Fig. 7. The fermion propagator with the insertion of g/N is nothing else than the first-order perturbative correction by the contact four-fermion interaction. We can then pick this constant term out of the one-boson-loop diagram and add it to the one-fermion-loop MF graph contributing to $\mathcal{D}_0^{-1}(0)$, where it is absorbed in the perturbative renormalization of the Fermi energy [62].

C. Results

Recalling finally from the BCS theory that at temperature T different from the MF critical temperature $T_c^{(0)}$, $\mathcal{D}_0^{-1}(0)$ is equal to $\mathcal{N} \log(T/T_c^{(0)})$, setting $\mathcal{D}^{-1}(0)$ to zero leads to the following compact formula for the critical temperature,

$$T_c = T_c^{(0)} \exp \left[-\frac{N_B}{N_F} X \left(\frac{T_c^{(0)}}{\mu} \right) \right], \quad (16)$$

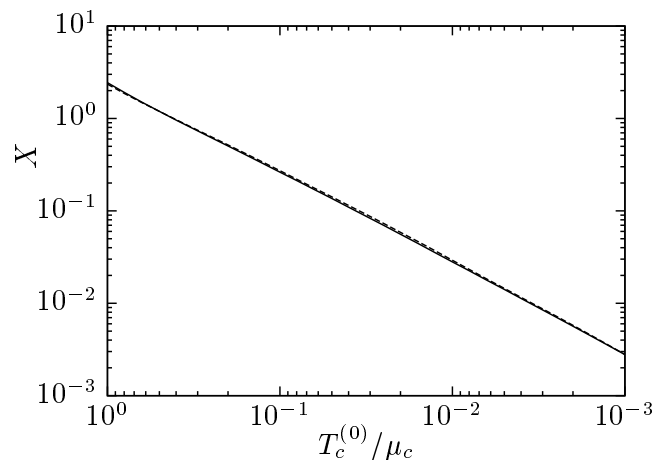


FIG. 9: Correction to the critical temperature calculated using the high-density approximation in the *ultrarelativistic limit*. The calculation was done with the cutoff on fermion energy variable set to $2T_c^{(0)}$ (solid line) and $4T_c^{(0)}$ (dashed line).

where X is a dimensionless function (different in the two limits), given by the integral in Eq. (15) in the dimensionless variables introduced above.

Eq. (16) constitutes our final result regarding relativistic superconductors, written in the most general form: The coupling constant is completely eliminated in favor of the MF ratio $T_c^{(0)}/\mu$. Also, the specific form of the pairing channel only enters through the algebraic factor N_B/N_F .

Two comments are in order here. First, Eq. (16) gives the correction to the critical temperature at fixed chemical potential; we do not solve the number equation along with the Thouless criterion to obtain a result at fixed density. In the context of color-superconducting quark matter, the (baryon number) chemical potential is usually treated as a free parameter. In fact, it is a more suitable parameter than the density itself in the case that the phase diagram involves first-order phase transitions, where the density becomes discontinuous.

Second, the $1/N$ algorithm based on Eq. (5) (reduced to a one-variable problem by fixing the chemical potential) would suggest to interpret the exponent in Eq. (16) as the relative change of the critical temperature, or minus the relative change of the inverse critical temperature, depending on the choice of variable. In this section, we used the $1/N$ expansion to derive Eq. (15) as the one-loop corrected Thouless criterion, and to evaluate the loop correction at the MF value of the critical temperature. We now go slightly beyond the $1/N$ philosophy in the sense that our result, Eq. (16), does not need any further expansion and defines the critical temperature T_c in an unambiguous manner. The value of T_c thus calculated is always positive, no matter how large the loop function X is. (Of course, we would still consider the used approximation unreliable once X becomes of order

one or larger.) In addition, the temperature correction does not display a finite offset in the BCS limit, as found in Sec. II and assigned to the $1/N$ expansion as an artifact. On the contrary, it drops rapidly with decreasing ratio $T_c^{(0)}/\mu$, as one would naively expect [63].

To complete the discussion of the results, we show in Figs. 8 and 9 the numerically calculated values of the function X in the NR and UR limits, respectively. For $T_c^{(0)}/\mu$ smaller than about 0.1 the functions may be very well approximated by a simple empirical power law,

$$X_{\text{NR}}\left(\frac{T_c^{(0)}}{\mu}\right) \approx 5.2\frac{T_c^{(0)}}{\mu}, \quad X_{\text{UR}}\left(\frac{T_c^{(0)}}{\mu}\right) \approx 2.8\frac{T_c^{(0)}}{\mu}, \quad (17)$$

which can be used for a fast rough estimate of the size of fluctuation effects.

D. Possible impact on QCD phase diagram

Finally, we wish to illustrate a possible impact of fluctuations on the QCD phase diagram. In Fig. 10 we display the phase diagrams from a simple NJL-model calculation; the model is the same one as adopted in Ref. [52] with the diquark coupling G_d chosen such that the CFL gap is 50 MeV at $\mu = 500$ MeV in the chiral SU(3) limit. Fig. 10 (a) shows the phase diagram at vanishing strange quark mass, i.e., in the chiral SU(3) limit. The dashed line is the critical temperature at the leading order in $1/N$ expansion, and the suppression of the critical temperature due to fluctuation effects at NLO is included by means of the analytic formula (16). Interestingly, because $N_B/N_F = 1$ in the CFL case while it is just $1/2$ in the 2SC phase, we expect a finite region with 2SC pairing below the normal phase even in the chiral SU(3) limit.

However, since the approximation which led to Eq. (16) is only valid in the high-density regime where $T_c^{(0)}/\mu$ is small, we have to keep in mind that the estimates are not quantitative at low density. It is also important to note that we derived the shift of critical temperature of the CFL phase, taking into account the fluctuations in the normal phase. Now that we know that the 2SC phase interposes between the normal and CFL phases, it would be more appropriate to somehow take into account the fluctuations within the 2SC phase for a more realistic estimate of the temperature of the phase transition between the CFL and 2SC phases.

Fig. 10 (b) shows the phase diagram at a finite strange quark mass, but without quantum fluctuation effects. The strange quark mass is set to $M_s = 200$ MeV, and is for simplicity treated as an external parameter rather than a dynamical one. Also, the intricate charge neutrality effects are ignored here because they are not important for our purposes; we just remark that the charge neutrality constraints bring fine splittings to the T_c 's resulting in the appearance of tiny regions with dSC or uSC pairing [52, 53]. Comparing the two plots, we can

see that the quantum fluctuation effects may play a significant role at high density which may be similar to that of the strange quark mass. This can be understood in a model-independent way as follows. Within a weak-coupling Ginzburg–Landau approach, it was shown that the strange quark mass and charge neutrality result in shifts in the melting temperatures T_i of the order parameters Δ_i of the CFL phase of the order [53]

$$\frac{\delta T_i}{T_c^{(0)}} \sim -\frac{M_s^2}{8\mu^2} \log\left(\frac{\mu}{T_c^{(0)}}\right).$$

These corrections die rapidly as $(M_s/\mu)^2$ at large μ , while the correction to $T_c^{(0)}$ from order parameter fluctuations prevails as it behaves asymptotically like $T_c^{(0)}/\mu$. Considering in addition the fact that M_s is a decreasing function of μ whereas the superconducting gap turns out to increase as $\mu \rightarrow \infty$ [54, 55], we conclude that the quantum fluctuation is more important than the effect of a strange quark mass at high density.

In a more realistic situation, there would be another source of fluctuations from thermal configurations of gauge fields [56] which makes the superconducting–normal transition first order. The shift of the critical temperature turns out to be positive and is estimated to be proportional to the QCD coupling g in the weak-coupling regime [56]. Therefore, in realistic quark matter the order parameter and gauge field fluctuations will compete each other. This issue certainly deserves a further study in future.

IV. SUMMARY AND CONCLUSIONS

We have investigated the $1/N$ expansion for strongly interacting Fermi systems, proposed recently [16, 17]. We first studied in detail the case of nonrelativistic Fermi gas near unitarity, extending the previous results by the calculation of the critical temperature off the unitarity. Even though the $1/N$ expansion can give a result for the critical temperature at unitarity which is very close to the prediction from Monte Carlo simulations [21, 22], there is an inherent ambiguity due to the choice of observable to generate (and truncate) the $1/N$ series. This ambiguity makes the $1/N$ expansion in the current setting useless when the corrections to the MF theory are large, in particular on the BEC side of the crossover.

We paid particular attention to the evolution of the fluctuation corrections in the BCS regime, where they are expected to be small, and the $1/N$ series thus to converge fast. We showed that the next-to-leading order in the $1/N$ expansion reproduces the well-known perturbative correction to the chemical potential up to second order. As far as the critical temperature is concerned, the fluctuation correction indeed decreases at weak coupling, but leaves a finite offset in the $k_F a \rightarrow 0$ – limit. We argued that this is likely to be an artifact of the $1/N$ expansion.

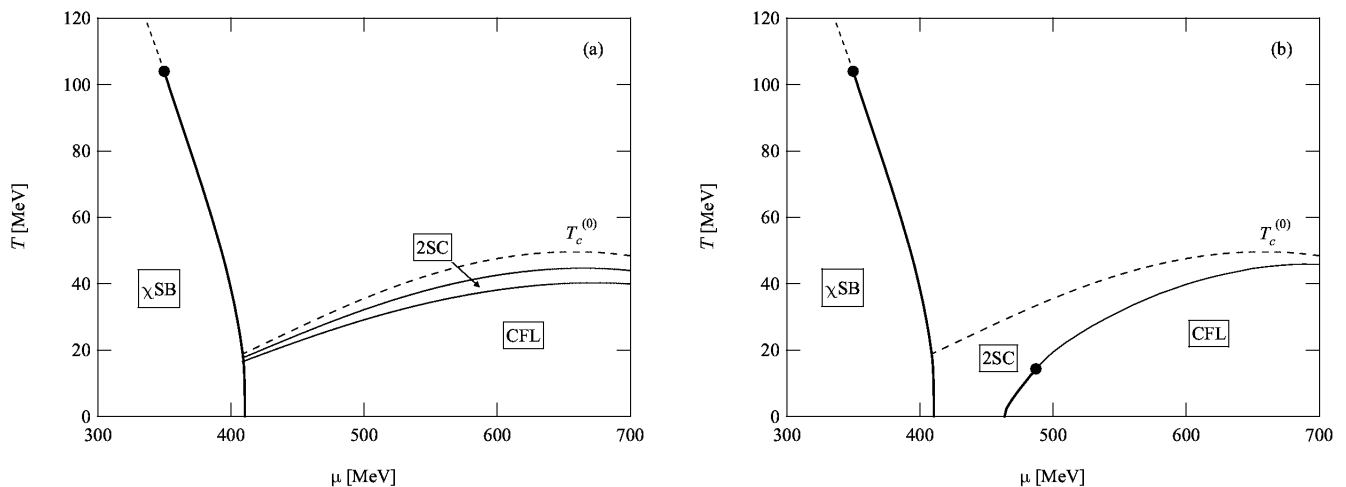


FIG. 10: (a) Phase diagram at vanishing strange quark mass $M_s = 0$ but *with* quantum fluctuation effects. (b) The same phase diagram for $M_s = 200$ MeV *without* fluctuation effects. $T_c^{(0)}$ is the critical temperature at the leading order in $1/N$.

In Sec. III we applied the idea to strongly coupled relativistic superconductors, having in mind in particular color-superconducting dense quark matter. We used a simple class of NJL-type models and resorted to a high-density approximation in order to avoid conceptual difficulties associated with renormalization and entanglement of several energy scales. Our results are summarized in Eqs. (16) and (17) and Figures 8 and 9. They are physically intuitive in the sense that the fluctuation corrections are small in the BCS limit, decreasing linearly with the ratio $T_c^{(0)}/\mu$, i.e., exponentially with the inverse coupling, and become large as $T_c^{(0)}/\mu$ approaches the order of 0.1 and further grows.

In particular for typical color superconductors, the corrections to critical temperature are expected to be as large as tens percent. Another important conclusion is that, within the simple setting used here, the fluctuation corrections are expressed as a universal function of the dimensionless ratio $T_c^{(0)}/\mu$. The whole dependence on the symmetry structure of the pairing is encoded in an algebraic prefactor, which counts the number of bosonic and fermionic degrees of freedom. This makes it straightforward to compare the effects for different competing superconducting phases, and thus estimate the impact of the order parameter fluctuations on the phase diagram such as in Fig. 10. Upon this investigation of the fluctu-

ation corrections within a simple model, we plan, in our future work, to include the effects of chemical potential mismatch and color neutrality in order to obtain a more realistic description of quark matter.

Finally, we would like to stress the conceptual simplicity of this approach to order parameter fluctuations. We do not need to solve a complicated set of self-consistent integral equations like in other techniques going beyond the MF approximation, such as the Cornwall–Jackiw–Tomboulis one. Instead, one just has to evaluate a single multidimensional sum-integral. We therefore believe that the $1/N$ expansion may provide an efficient tool to determine the fluctuation effects in such strongly-coupled systems as, for instance, the color superconductors.

Acknowledgments

The authors are grateful to J. Hošek and D. H. Rischke for fruitful discussions. The present work was supported by the Alexander von Humboldt Foundation. Numerical calculations were performed using the facilities of the Frankfurt Center for Scientific Computing, and in part on Altix3700 at the Yukawa Institute for Theoretical Physics of Kyoto University.

-
- [1] D. M. Eagles, Phys. Rev. **186**, 456 (1969).
 [2] A. J. Leggett, J. Phys. Colloques **41**, 19 (1980).
 [3] P. Nozières and S. Schmitt-Rink, J. Low Temp. Phys. **59**, 195 (1985).
 [4] C. A. Regal, M. Greiner, and D. S. Jin, Phys. Rev. Lett. **92**, 040403 (2004), cond-mat/0401554.
 [5] M. Bartenstein, A. Altmeyer, S. Riedl, S. Jochim,

- C. Chin, J. Hecker Denschlag, and R. Grimm, Phys. Rev. Lett. **92**, 120401 (2004), cond-mat/0401109.
 [6] M. W. Zwierlein, C. A. Stan, C. H. Schunck, S. M. F. Raupach, A. J. Kerman, and W. Ketterle, Phys. Rev. Lett. **92**, 120403 (2004), cond-mat/0403049.
 [7] T. Bourdel, L. Khaykovich, J. Cubizolles, J. Zhang, F. Chevy, M. Teichmann, L. Tarruell, S. J. J. M. F.

- Kokkelmans, and C. Salomon, Phys. Rev. Lett. **93**, 050401 (2004), cond-mat/0403091.
- [8] D. T. Son, Phys. Rev. **D78**, 046003 (2008), arXiv:0804.3972 [hep-th].
- [9] K. Balasubramanian and J. McGreevy, Phys. Rev. Lett. **101**, 061601 (2008), arXiv:0804.4053 [hep-th].
- [10] R. Haussmann, Phys. Rev. **B49**, 12975 (1994).
- [11] R. Haussmann, W. Rantner, S. Cerrito, and W. Zwirger, Phys. Rev. **A75**, 023610 (2007), cond-mat/0608282.
- [12] H. Heiselberg, Phys. Rev. **A63**, 043606 (2001), cond-mat/0002056.
- [13] Z. Nussinov and S. Nussinov, Phys. Rev. **A74**, 053622 (2006), cond-mat/0410597.
- [14] Y. Nishida and D. T. Son, Phys. Rev. Lett. **97**, 050403 (2006), cond-mat/0604500.
- [15] J.-W. Chen and E. Nakano, Phys. Rev. **A75**, 043620 (2007), cond-mat/0610011.
- [16] P. Nikolić and S. Sachdev, Phys. Rev. **A75**, 033608 (2007).
- [17] M. Y. Veillette, D. E. Sheehy, and L. Radzihovsky, Phys. Rev. **A75**, 043614 (2007).
- [18] Q. Chen, J. Stajic, S. Tan, and K. Levin, Phys. Rept. **412**, 1 (2005).
- [19] J. Carlson, S.-Y. Chang, V. R. Pandharipande, and K. E. Schmidt, Phys. Rev. Lett. **91**, 050401 (2003), physics/0303094.
- [20] A. Bulgac, J. E. Drut, and P. Magierski, Phys. Rev. Lett. **96**, 090404 (2006), cond-mat/0505374.
- [21] E. Burovski, N. Prokof'ev, B. Svistunov, and M. Troyer, Phys. Rev. Lett. **96**, 160402 (2006), cond-mat/0602224.
- [22] E. Burovski, E. Kozik, N. Prokof'ev, B. Svistunov, and M. Troyer, Phys. Rev. Lett. **101**, 090402 (2008), arXiv:0805.3047 [cond-mat.str-el].
- [23] Y. Nambu and G. Jona-Lasinio, Phys. Rev. **122**, 345 (1961).
- [24] Y. Nambu and G. Jona-Lasinio, Phys. Rev. **124**, 246 (1961).
- [25] B. C. Barrois, Nucl. Phys. **B129**, 390 (1977).
- [26] S. C. Frautschi (1980), in Workshop on Hadronic Matter at Extreme Energy Density, Erice, Italy, Oct 13-21, 1978.
- [27] M. G. Alford, A. Schmitt, K. Rajagopal, and T. Schaefer (2007), arXiv:0709.4635 [hep-ph].
- [28] E. Babaev, Int. J. Mod. Phys. **A16**, 1175 (2001), hep-th/9909052.
- [29] M. Matsuzaki, Phys. Rev. **D62**, 017501 (2000), hep-ph/9910541.
- [30] H. Abuki, T. Hatsuda, and K. Itakura, Phys. Rev. **D65**, 074014 (2002), hep-ph/0109013.
- [31] M. Kitazawa, T. Koide, T. Kunihiro, and Y. Nemoto, Phys. Rev. **D70**, 056003 (2004), hep-ph/0309026.
- [32] K. Nawa, E. Nakano, and H. Yabu, Phys. Rev. **D74**, 034017 (2006), hep-ph/0509029.
- [33] M. Kitazawa, D. H. Rischke, and I. A. Shovkovy, Phys. Lett. **B663**, 228 (2008), arXiv:0709.2235 [hep-ph].
- [34] Y. Nishida and H. Abuki, Phys. Rev. **D72**, 096004 (2005), hep-ph/0504083.
- [35] H. Abuki, Nucl. Phys. **A791**, 117 (2007), hep-ph/0605081.
- [36] J. Deng, A. Schmitt, and Q. Wang, Phys. Rev. **D76**, 034013 (2007), nucl-th/0611097.
- [37] L. He and P. Zhuang, Phys. Rev. **D75**, 096003 (2007), hep-ph/0703042.
- [38] G.-F. Sun, L. He, and P. Zhuang, Phys. Rev. **D75**, 096004 (2007), hep-ph/0703159.
- [39] T. Brauner, Phys. Rev. **D77**, 096006 (2008), arXiv:0803.2422 [hep-ph].
- [40] B. Chatterjee, H. Mishra, and A. Mishra (2008), arXiv:0804.1051 [hep-ph].
- [41] L. He and P. Zhuang, Phys. Rev. **D76**, 056003 (2007), arXiv:0705.1634 [hep-ph].
- [42] J. M. Cornwall, R. Jackiw, and E. Tomboulis, Phys. Rev. **D10**, 2428 (1974).
- [43] J. Deng, J.-c. Wang, and Q. Wang, Phys. Rev. **D78**, 034014 (2008), arXiv:0803.4360 [hep-ph].
- [44] C. A. R. Sa de Melo, M. Randeria, and J. R. Engelbrecht, Phys. Rev. Lett. **71**, 3202 (1993).
- [45] R. B. Diener, R. Sensarma, and M. Randeria, Phys. Rev. **A77**, 023626 (2008), arXiv:0709.2653 [cond-mat.other].
- [46] A. L. Fetter and J. D. Walecka, *Quantum theory of many-particle systems*, International series in pure and applied physics (McGraw-Hill, New York, 1971).
- [47] R. J. Furnstahl and H. W. Hammer, Annals Phys. **302**, 206 (2002), nucl-th/0208058.
- [48] D. J. Thouless, Ann. Phys. (N.Y.) **10**, 553 (1960).
- [49] G. Nardulli, Riv. Nuovo Cim. **25N3**, 1 (2002), hep-ph/0202037.
- [50] D. Bailin and A. Love, Phys. Rept. **107**, 325 (1984).
- [51] R. D. Pisarski and D. H. Rischke, Phys. Rev. **D61**, 074017 (2000), nucl-th/9910056.
- [52] H. Abuki and T. Kunihiro, Nucl. Phys. **A768**, 118 (2006), hep-ph/0509172.
- [53] K. Iida, T. Matsuura, M. Tachibana, and T. Hatsuda, Phys. Rev. Lett. **93**, 132001 (2004), hep-ph/0312363.
- [54] D. T. Son, Phys. Rev. **D59**, 094019 (1999), hep-ph/9812287.
- [55] T. Schaefer and F. Wilczek, Phys. Rev. **D60**, 114033 (1999), hep-ph/9906512.
- [56] I. Giannakis, D.-F. Hou, H.-C. Ren, and D. H. Rischke, Phys. Rev. Lett. **93**, 232301 (2004), hep-ph/0406031.
- [57] L. P. Gorkov and T. K. Melik-Barkhudarov, Sov. Phys. JETP **13**, 1018 (1961).
- [58] R. J. Furnstahl, H. W. Hammer, and S. J. Puglia, Annals Phys. **322**, 2703 (2007), nucl-th/0612086.
- [59] It was argued in Ref. [16] that due to the distinct physical origin of the LO (fermions) and NLO (bosons) contribution to the thermodynamic potential, their relative size should not be used to test the accuracy of the $1/N$ expansion. This postpones the issue of convergence of the series to higher orders, yet the ambiguity encountered at NLO remains.
- [60] Strictly speaking, our calculation differs from the original NSR theory [3] in that we perform the Matsubara sum in the one-loop contribution to the number density directly while it is more conventional to make analytic continuation to the real frequencies and use spectral representation. Of course, the results should coincide as long as the analytic continuation has been done properly.
- [61] Should we include several pairing channels, our results would naturally generalize, giving a different fluctuation effect for each of them even in the normal phase.
- [62] Actually, the first-order perturbative renormalization of the fermion propagators in the fermion loop in $\mathcal{D}_0^{-1}(0)$ produces two equal terms, one from each propagator. However, this is exactly what we need because the loop diagram, being symmetric, carries a symmetry factor $\frac{1}{2}$.
- [63] As shown by Gorkov and Melik-Barkhudarov, particle-hole fluctuations lead to a suppression of the gap and critical temperature even in the BCS limit [57, 58]. We do

not expect this effect to be reproduced by our calculation since it includes only pair fluctuations [45].